Gazi Üniversitesi
Fen Bilimleri Dergisi
PART C: TASARIM VE TEKNOLOJİ

Gazi University
Journal of Science
PART C: DESIGN AND TECHNOLOGY

GU J Sci, Part C, 14(1): 506-515 (2026)

Structure–Defect–Interface Engineering in 3% Sn-Doped ZnO Thin Films for Enhanced n–Si Schottky Diode Performance

Erman ÇOKDUYGULULAR[1*]

[1]*Istanbul University-Cerrahpaşa, Faculty of Engineering, Department of Engineering Sciences, TR-34320, Istanbul/ Türkiye*

Article Info

Research article
Received: 31/01/2026
Revision: 24/02/2026
Accepted: 25/02/2026

Keywords

Sn-doped ZnO thin films
Capacitance-voltage analysis
Frequency-dependent electrical characteristics
RF magnetron co-sputtering

Makale Bilgisi

Araştırma makalesi
Başvuru: 31/01/2026
Düzeltme: 24/02/2026
Kabul: 25/02/2026

Anahtar Kelimeler

Sn-katkılı ZnO ince filmler
Kapasitans-gerilim analizi
Frekansa bağlı elektriksel özellikler
RF magnetron eş-püskürtme

Graphical/Tabular Abstract (Grafik Özet)

Structural, defect, and interface engineering in 3% Sn-doped ZnO thin films enhanced Schottky barrier height, reduced series resistance, suppressed deep-level emission, and improved rectifying performance in Au/ZnO:Sn/n–Si devices. / %3 Sn katkılı ZnO ince filmlerde yapısal, kusur ve arayüz mühendisliği, Au/ZnO:Sn/n–Si Schottky diyotlarında bariyer yüksekliğini artırmış, seri direnci azaltmış, derin seviye emisyonunu baskılamış ve doğrultucu performansı iyileştirmiştir.

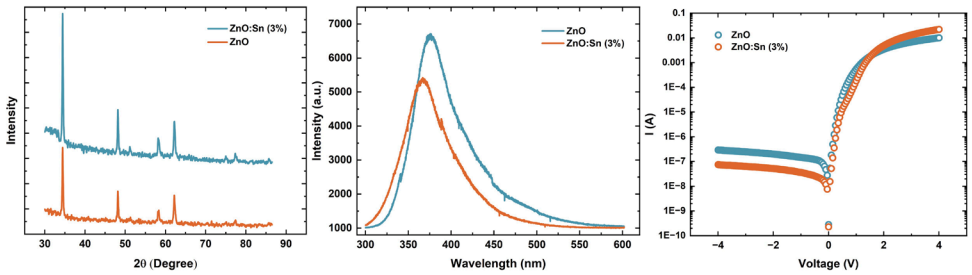


***Figure A**: Structural, optical, and electrical characteristics of undoped and 3% Sn-doped ZnO thin films and Au/ZnO/n–Si Schottky structures. / **Şekil A:** Katkısız ve %3 Sn katkılı ZnO ince filmlerin ve Au/ZnO/n–Si Schottky yapılarının yapısal, optik ve elektriksel özellikler.*

Highlights (Önemli noktalar)

- *Sn incorporation improved (002) preferential orientation and crystalline quality of ZnO thin films. / %3 Sn katkısı ZnO ince filmlerde (002) tercihli yönlenmeyi ve kristal kalitesini iyileştirmiştir.*
- *Sn doping increased Schottky barrier height and reduced series resistance in Au/ZnO/n–Si devices. / Sn katkısı Au/ZnO/n–Si diyotlarında Schottky bariyer yüksekliğini artırmış ve seri direnci azaltmıştır.*
- *Frequency-dependent C–V and G/ω analyses revealed stable depletion-region behavior and limited active interface-state response. / Frekansa bağlı C–V ve G/ω analizleri kararlı bir tükenim bölgesi davranışı ve sınırlı aktif arayüz durum yoğunluğu göstermiştir.*

***Aim (Amaç):** This study investigates the effect of 3% Sn incorporation on the structural, optical, and electrical properties of ZnO thin films and evaluates the performance of corresponding Au/ZnO/n–Si Schottky diodes. / Bu çalışma, ZnO ince filmlere %3 Sn katkısının yapısal, optik ve elektriksel özelliklere etkisini incelemekte ve karşılık gelen Au/ZnO/n–Si Schottky diyotlarının performansını değerlendirmektedir.*

***Originality (Özgünlük):** The study establishes a direct correlation between Sn-induced defect modulation, interface quality, and Schottky diode performance through integrated structural, optical, and frequency-dependent electrical analyses. / Çalışma, Sn katkısına bağlı kusur modülasyonu, arayüz kalitesi ve Schottky diyot performansı arasındaki doğrudan ilişkiyi bütüncül yapısal, optik ve frekansa bağlı elektriksel analizlerle ortaya koymaktadır.*

***Results (Bulgular):** Sn incorporation enhanced (002) orientation, suppressed deep-level emission, increased barrier height (0.676 eV), reduced series resistance (113 Ω), and improved rectification and frequency stability in Au/ZnO:Sn/n–Si devices. / Sn katkısı (002) yönlenmeyi artırmış, derin seviye emisyonunu baskılamış, bariyer yüksekliğini (0.676 eV) artırmış, seri direnci (113 Ω) azaltmış ve Au/ZnO:Sn/n–Si diyotlarında doğrultma ve frekans kararlılığını iyileştirmiştir.*

***Conclusion (Sonuç):** Controlled 3% Sn doping improves crystalline quality, reduces defect-related recombination, and significantly enhances Schottky junction performance, highlighting its potential for optoelectronic applications. / Kontrollü %3 Sn katkısı kristal kalitesini artırmakta, kusur kaynaklı yeniden birleşmeyi azaltmakta ve Schottky bağlantı performansını belirgin şekilde iyileştirerek optoelektronik uygulamalar için potansiyel sunmaktadır.*

*Corresponding author, e-mail: erman.cokduygulular@iuc.edu.tr
DOI: 10.29109/gujsc.1878755

GU J Sci, Part C, 14(1): 506-515 (2026)

Gazi Üniversitesi
Fen Bilimleri Dergisi
PART C: TASARIM VE TEKNOLOJİ

Gazi University
Journal of Science
PART C: DESIGN AND TECHNOLOGY

http://dergipark.gov.tr/gujsc

Structure–Defect–Interface Engineering in 3% Sn-Doped ZnO Thin Films for Enhanced n–Si Schottky Diode Performance

Erman ÇOKDUYGULULAR[1*]

[1]*Istanbul University-Cerrahpaşa, Faculty of Engineering, Department of Engineering Sciences, TR-34320, Istanbul/ Türkiye*

Article Info

Research article
Received: 31/01/2026
Revision: 24/02/2026
Accepted: 25/02/2026

Keywords

Sn-doped ZnO thin films
Capacitance-voltage analysis
Frequency-dependent electrical characteristics
RF magnetron co-sputtering

Abstract

The influence of Sn incorporation on the structural, optical, and electrical performance of ZnO-based Schottky devices was systematically investigated. Undoped and 3% Sn-doped ZnO thin films were deposited on glass and n-type Si substrates by RF magnetron co-sputtering. X-ray diffraction confirmed a hexagonal wurtzite structure with a pronounced (002) preferred orientation, while Sn incorporation improved crystalline quality by increasing peak intensity and reducing microstrain. Photoluminescence analysis revealed enhanced near-band-edge emission and suppressed deep-level emission in the Sn-doped film, indicating reduced defect-related recombination. UV–Visible measurements demonstrated high optical transmittance in the visible region and slight modification of the optical band structure upon Sn doping. Current–voltage measurements verified Schottky-type rectifying behavior in both Au/ZnO/n–Si and Au/ZnO:Sn (3%)/n–Si structures, with the Sn-doped device exhibiting a higher barrier height, lower series resistance, an improved ideality factor, and enhanced forward current conduction. Capacitance–voltage and conductance–voltage analyses performed on the Sn-doped structure (50 kHz–1 MHz) indicated stable depletion-region behavior and limited active interface-state response. These results confirm that controlled Sn incorporation enhances crystalline integrity, defect modulation, and Schottky junction performance in ZnO thin films, supporting their applicability in UV detection and optoelectronic rectifier applications.

Geliştirilmiş n–Si Schottky Diyot Performansı için %3 Sn Katkılı ZnO İnce Filmlerde Yapı–Kusur–Arayüz Mühendisliği

Makale Bilgisi

Araştırma makalesi
Başvuru: 31/01/2026
Düzeltme: 24/02/2026
Kabul: 25/02/2026

Anahtar Kelimeler

Sn-katkılı ZnO ince filmler
Kapasitans-gerilim analizi
Frekansa bağlı elektriksel özellikler
RF magnetron eş-püskürtme

Öz

Sn katkısının ZnO tabanlı Schottky aygıtların yapısal, optik ve elektriksel performansı üzerindeki etkisi sistematik olarak incelenmiştir. Katkısız ve %3 Sn katkılı ZnO ince filmler, RF magnetron eş-püskürtme yöntemiyle cam ve n-tipi Si altlıklar üzerine biriktirilmiştir. X-ışını kırınımı analizleri, belirgin bir (002) tercihli yönlenmeye sahip hekzagonal wurtzit yapıyı doğrulamış; Sn katkısının pik şiddetini artırarak ve mikrogerinimi azaltarak kristal kalitesini iyileştirdiğini göstermiştir. Fotolüminesans analizleri, Sn katkılı filmde bant kenarı emisyonunun güçlendiğini ve derin seviye emisyonunun baskılandığını ortaya koymuş, bu durum kusur kaynaklı yeniden birleşmenin azaldığını göstermiştir. UV–Görünür bölge ölçümleri, görünür bölgede yüksek optik geçirgenlik ve Sn katkısına bağlı olarak optik bant yapısında hafif bir değişim olduğunu göstermiştir. Akım–gerilim ölçümleri, hem Au/ZnO/n–Si hem de Au/ZnO:Sn (%3)/n–Si yapılarında Schottky tipi doğrultucu davranışı doğrulamış; Sn katkılı aygıtta daha yüksek bariyer yüksekliği, daha düşük seri direnç, iyileştirilmiş idealite faktörü ve artmış ileri yön akım iletimi gözlenmiştir. Sn katkılı yapı üzerinde gerçekleştirilen kapasite–gerilim ve iletkenlik–gerilim analizleri (50 kHz–1 MHz), kararlı bir tükenim bölgesi davranışı ve sınırlı aktif arayüz durum tepkisi göstermiştir. Elde edilen sonuçlar, kontrollü Sn katkısının ZnO ince filmlerde kristal bütünlüğü, kusur modülasyonu ve Schottky bağlantı performansını iyileştirdiğini ve bu yapıların UV algılama ile optoelektronik doğrultucu uygulamaları için uygunluğunu desteklediğini doğrulamaktadır.

1. INTRODUCTION (GİRİŞ)

Zinc oxide (ZnO), an II–VI group semiconductor, has attracted significant attention owing to its wide direct band gap (3.2–3.37 eV), large exciton binding energy (~60 meV), chemical stability, and radiation hardness [1]. These intrinsic properties make ZnO suitable for ultraviolet (UV) photodetectors, gas sensors, photocatalysts, transparent electronics, and Schottky-type rectifying devices [1–6]. The

*Corresponding author, e-mail: erman.cokduygulular@iuc.edu.tr
DOI: 10.29109/gujsc.1878755

electrical conductivity and luminescence characteristics of ZnO are strongly governed by intrinsic point defects such as oxygen vacancies (V_O), zinc interstitials (Zn_i), and oxygen interstitials (O_i), as well as surface adsorbates, which play a decisive role in defect-related emission and carrier transport [2]. Therefore, controlled defect engineering and carrier-concentration modulation are essential for improving the performance of ZnO-based devices.

Extrinsic doping is widely employed to tailor ZnO properties. Among various dopants, tin (Sn) has emerged as an effective n-type dopant due to its ability to substitute for Zn^{2+} sites as Sn^{4+}, thereby introducing shallow donor levels and increasing the free-carrier concentration [7–11]. Several studies have reported that Sn incorporation modifies lattice parameters, crystallite size, strain, and preferential orientation in ZnO thin films [8,9,12]. In particular, enhanced (002) preferential orientation and improved crystallinity upon Sn doping have been observed in sputtered and solution-grown films [13,14]. Modified defect distributions and improved film densification often accompany these structural changes. Beyond structural effects, Sn doping significantly influences the optical and electronic properties of ZnO. Band-gap modulation associated with the Burstein–Moss effect and defect-related band-gap renormalization has been reported in Sn-doped ZnO systems [10,15]. Suppression of deep-level emission (DLE) and reduced carrier recombination have been demonstrated in Sn-doped ZnO thin films, indicating effective defect passivation and improved optical quality [15,16]. Furthermore, enhanced photocatalytic and photoelectrochemical performance has been attributed to improved charge-separation efficiency and reduced recombination losses in Sn-modified ZnO systems [3,5,15].

Thin film deposition techniques, particularly radio frequency (RF) magnetron sputtering, enable precise control over composition, thickness, and crystallographic orientation, making them highly suitable for device-oriented ZnO fabrication [17]. Sn-doped ZnO thin films have been explored for UV photodetectors [13], gas sensing applications [17], and optoelectronic devices [4,16]. Although these studies clearly demonstrate that Sn incorporation enhances structural and optical properties, most investigations primarily emphasize photocatalytic efficiency, sensing response, or optical characteristics rather than comprehensive Schottky diode behavior. Despite the extensive literature on Sn-doped ZnO systems, systematic and quantitative investigations correlating structural evolution, defect-related optical behavior, and Schottky interface dynamics (including current–voltage (I–V) characteristics and frequency-dependent capacitance–voltage (C–V) and conductance–voltage (G/ω–V) analyses) in sputter-grown Sn-doped ZnO thin films remain limited. In particular, the interplay between Sn-induced defect modulation and metal–semiconductor interface characteristics has not been sufficiently clarified within a unified experimental framework.

In this context, the present study systematically investigates the influence of 3% Sn incorporation on the structural, optical, and electrical characteristics of ZnO thin films deposited via RF magnetron co-sputtering. By integrating X-ray diffraction (XRD), photoluminescence (PL), UV–Visible (UV–Vis) spectroscopy, current–voltage (I–V), capacitance–voltage, and conductance–voltage analyses, this work establishes a comprehensive structure–defect–device performance relationship in Au/ZnO/n–Si and Au/ZnO:Sn (3%)/n–Si Schottky structures. The findings provide quantitative insight into defect engineering and interface modulation in Sn-doped ZnO thin films and contribute to the development of high-performance ZnO-based optoelectronic and rectifying devices.

2. MATERIALS AND METHODS (MATERYAL VE METOD)

2.1. Experimental Equipment (Deneysel Ekipman)

The main purpose of this study is to determine the effects of processing parameters on the completeness of the measurement in the process of machining the keyseat with EDM to the Ti-6Al-4V alloy. In this study, Ti-4Al-6V titanium alloy with a diameter of 14 mm was used as the workpiece material. For the specified diameter, the DIN 6885 standard is set to be keyseat dimensions width (b) 5mm, depth (h) 5mm, keyseat depth (t1) 3mm and length (L) 20mm. Keyseat sizes according to DIN 6885 standard are given in Figure 1.

Undoped and 3% Sn-doped ZnO thin films were produced using a radio frequency (RF) magnetron sputtering system. The undoped ZnO films were fabricated employing a high–purity ZnO ceramic target (99.99%). Conversely, Sn–doped ZnO thin films were synthesized under identical deposition parameters through the co–sputtering of ZnO and Sn targets. The Sn doping concentration was controlled at roughly 3 at—% by meticulously regulating the power ratio between the ZnO and Sn targets.

The thin films were deposited onto two different types of substrates, depending on the intended characterization techniques:

(i) optically transparent glass substrates for X-ray diffraction (XRD), photoluminescence (PL), and UV–Vis measurements,

(ii) (100)-oriented boron-doped n–type Si substrates for electrical characterizations, including current–voltage (I–V), capacitance–voltage (C–V), and conductance/angular frequency–voltage (G/ω–V) analyses.

The structural properties of the ZnO and Sn-doped ZnO thin films were examined by XRD using a Bruker D8 Advance diffractometer operated in the diffraction angle range of $30° \leq 2\theta \leq 80°$ with a step size of 0.01°. Room–temperature PL spectra were recorded using a Jobin Yvon Florog-550 PL system with a 50 mW He–Cd laser (λ = 325 nm) as an excitation light source. In addition, the optical properties of the thin films deposited on glass substrates were characterized by measuring their transmittance spectra using a Lambda 2S UV–Vis spectrophotometer.

For the electrical characterization of the Au/ZnO/n–Si and Au/ZnO:Sn (3%)/n–Si structures, Schottky diode configurations were fabricated on n–type Si substrates. Prior to the formation of the front Schottky contacts, a 150 nm thick Au layer (99.9% purity) was deposited onto the back surface of the n–Si substrates using a thermal evaporation system to form an ohmic contact. The back contact was subsequently ohmicized by annealing the samples in a rapid thermal annealing (RTA) system at 350 °C for 3 min under vacuum conditions. Following this process, circular Au Schottky contacts with a thickness of 150 nm and a diameter of 1 mm were deposited onto the ZnO and Sn–doped ZnO thin film surfaces at room temperature using a shadow mask in the same thermal evaporation system. The current–voltage characteristics of both Au/ZnO/n–Si and Au/ZnO:Sn (3%)/n–Si Schottky diodes were measured at room temperature using a Keithley 4200 semiconductor characterization system. C–V and G/ω–V analyses were performed only for the Au/ZnO:Sn (3%)/n–Si structure over the frequency range of 50 kHz to 1 MHz under an applied bias of ±4 V using an HP 4192A LF impedance analyzer.

3. RESULTS (BULGULAR)

3.1. Structural and Optical Properties (Yapısal ve Optik Özellikler)

Figure 1 presents the XRD patterns of undoped and 3% Sn-doped ZnO thin films. All diffraction peaks can be indexed to the hexagonal wurtzite ZnO structure (JCPDS No. 36-1451), confirming the formation of single-phase ZnO without detectable secondary phases. No diffraction peaks corresponding to metallic Sn, SnO, or SnO_2 are observed, indicating successful incorporation of Sn ions into the ZnO lattice. Similar phase preservation at low and moderate Sn doping levels has been reported in previous studies [9,11,12], in which substitutional incorporation of Sn^{4+} or Sn^{2+} into Zn^{2+} sites was observed without secondary phase formation. Both films exhibit a pronounced (002) diffraction peak, indicating strong c-axis preferential orientation perpendicular to the substrate. Such orientation is commonly observed in sputtered ZnO thin films, as growth along the (002) direction minimizes surface energy and stabilizes the wurtzite structure [17]. Notably, the (002) peak intensity increases and its full width at half maximum decreases upon Sn incorporation, suggesting improved crystallinity and enlarged crystallite size. Similar enhancements in (002) orientation and crystalline quality with Sn doping have been reported in ZnO:Sn films prepared by sputtering and sol–gel techniques, where dopant incorporation promotes lattice ordering and reduces structural defects [9,12]. The preservation of the wurtzite phase, along with peak sharpening and reduced lattice strain, indicates that 3% Sn incorporation improves the structural quality of ZnO thin films.

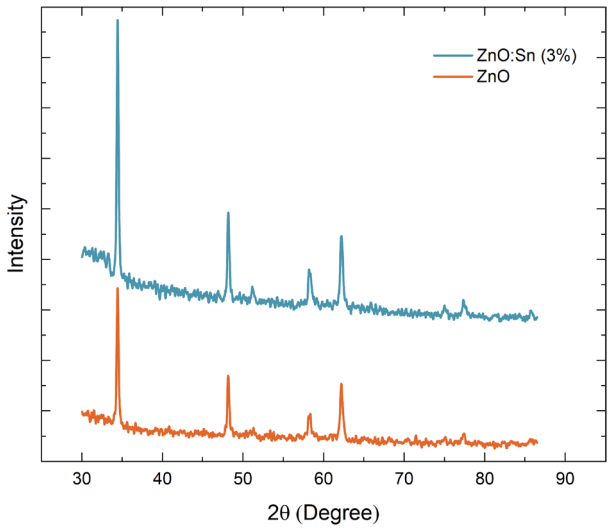


Figure 1. XRD results of ZnO (undoped and 3% Sn-doped) (ZnO'nun (katkısız ve %3 Sn katkılı) XRD sonuçları)

Figure 2 shows the PL spectra for both undoped ZnO and 3% Sn–doped ZnO thin films. Both samples exhibit a typical near–band–edge UV

emission, centered at 3.27 eV (~380 nm). This emission comes from excitons recombining in the hexagonal wurtzite ZnO lattice. In the visible range, a broad, deep–level emission band extending from about 450 to 650 nm is also observed. This emission is often linked to intrinsic point defects, such as oxygen vacancies (V_o), oxygen interstitials (O_i), and zinc interstitials (Zn_i).

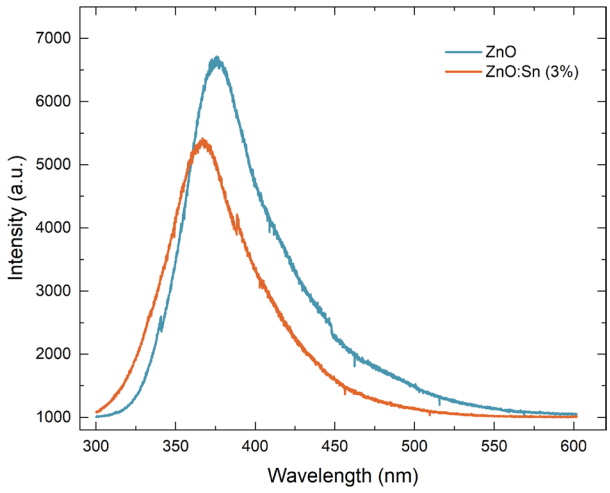


Figure 2. PL spectrum of ZnO (undoped and 3% Sn-doped) (ZnO'nun PL spektrumu (katkısız ve %3 Sn katkılı))

The PL spectra reveal the influence of 3% Sn incorporation through two primary features: a slight enhancement in the near-band-edge (NBE) emission and a pronounced suppression of the DLE band in the visible region. The reduced DLE intensity indicates a decrease in defect-related recombination centers, suggesting that Sn acts as a shallow donor and modifies the defect landscape of ZnO by mitigating intrinsic defect states, particularly those associated with oxygen vacancies. Similar defect-suppression behavior in Sn-doped ZnO has been reported in previous studies, where Sn incorporation reduced oxygen-vacancy-related emissions and improved overall

optical quality [9,11]. The observed PL behavior is consistent with the enhanced crystallinity inferred from XRD analysis, thereby supporting a direct correlation between structural refinement and defect modulation in the Sn-doped films.

The optical transmittance spectra of the films in the 300–900 nm range are shown in Figure 3. Both samples exhibit high transparency in the visible region, characteristic of wide-bandgap ZnO thin films deposited by sputtering [17]. The absorption edges are clearly observed in the near-UV region. Tauc plots derived from the absorption data indicate optical band gaps of approximately 3.31 eV for the undoped film and 3.33 eV for the 3% Sn-doped film, indicating a slight increase in the band gap upon Sn incorporation. This modest blue shift is primarily due to the Burstein–Moss effect, in which an increased carrier concentration shifts the Fermi level toward the conduction band, requiring higher photon energy for interband transitions. In addition, many-body interactions and band-gap renormalization may also contribute to the observed modification. Similar band structure variations in Sn-doped ZnO thin films have been reported in the literature, where the optical response was found to depend strongly on dopant concentration and carrier density [10,11].

Taken together, the XRD, PL, and UV–Vis results demonstrate that 3% Sn incorporation not only enhances crystalline quality but also modifies the defect structure and optical band characteristics of ZnO thin films, establishing a structural–optical correlation that directly influences subsequent device performance.

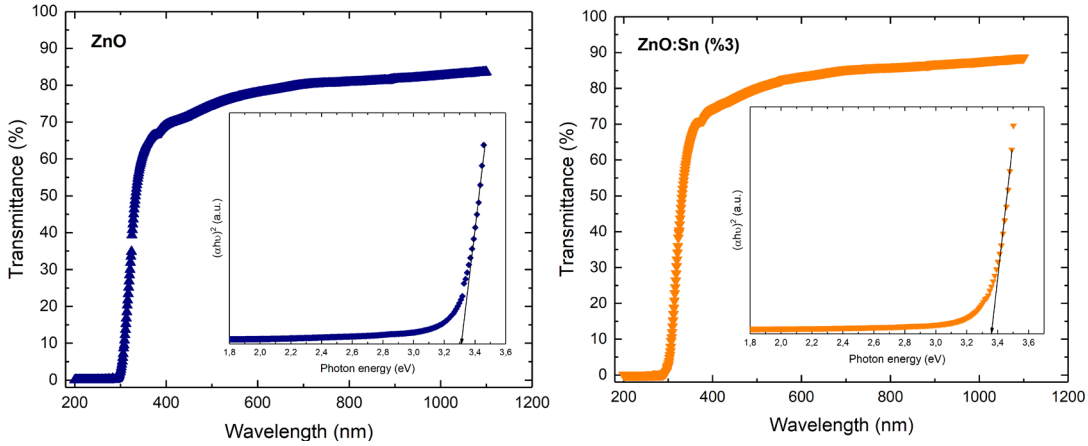


Figure 3. Optical transmittance spectra and corresponding Tauc plots of ZnO thin films (undoped and 3% Sn-doped), used to determine the optical band gap energies. (Optik bant aralığı enerjilerini belirlemek için kullanılan ZnO ince filmlerin (katkısız ve %3 Sn katkılı) optik geçirgenlik spektrumları ve karşılık gelen Tauc grafikleri)

3.2. Current–Voltage (I–V) Analysis (Akım-Gerilim (I-V) Analizi)

Figure 4 shows the I–V characteristics of the Au/ZnO/n–Si and Au/ZnO:Sn (3%)/n–Si Schottky diodes measured over a voltage range of ±4 V. Both structures exhibit clear rectifying behavior, confirming the successful formation of Schottky-type metal–semiconductor junctions. The incorporation of Sn into the ZnO layer significantly enhances the rectification characteristics, forward current density, and overall junction quality. Under forward bias, the Au/ZnO:Sn (3%)/n–Si device generates a higher current compared to the undoped counterpart. This enhancement can be attributed to the increased free-carrier concentration and improved bulk conductivity resulting from Sn^{4+} substitution for Zn^{2+} lattice sites, which introduces shallow donor levels and facilitates carrier transport across the metal–semiconductor interface.

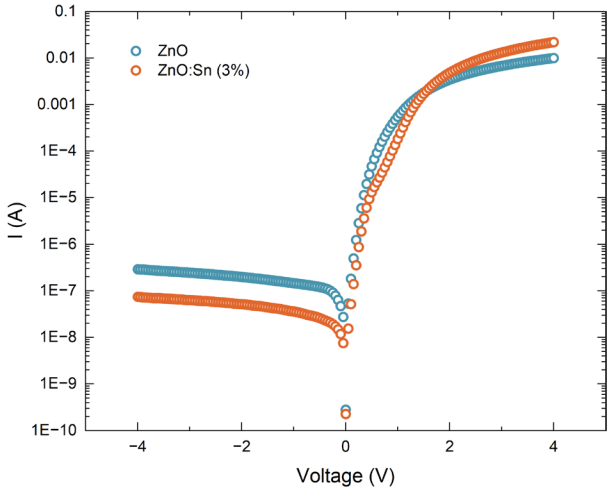


Figure 4. Current–voltage results of Au/ZnO/n-Si and Au/ZnO:Sn (3%)/n-Si Schottky diodes measured at room temperature (Oda sıcaklığında ölçülen Au/ZnO/n-Si ve Au/ZnO:Sn (3%)/n-Si Schottky diyotlarının akım-gerilim sonuçları)

In reverse bias, the Sn-doped device exhibits a notably lower leakage current, indicating a reduction in defect-related leakage pathways at the interface. The PL results, which show suppressed deep-level emissions, further support the reduction in defect-mediated recombination. Lower trap densities effectively minimize tunneling and recombination-assisted leakage currents under reverse bias conditions. The key diode parameters, including the series resistance (R_s), ideality factor (n), shunt resistance (R_{sh}), and barrier height (Φ_b), were extracted using the thermionic emission (TE) model and are summarized in Table 1.

The results indicate that Sn incorporation increases the shunt resistance by nearly one order of magnitude, demonstrating effective suppression of parallel leakage paths. Furthermore, the series resistance is significantly reduced in the Sn-doped device, reflecting improved carrier transport and enhanced conductivity within the ZnO layer. The extracted barrier height slightly increases with Sn addition, suggesting improved metal–semiconductor interface quality and reduced interface inhomogeneity.

Although the ideality factor values are greater than unity for both devices, indicating that recombination mechanisms and interface states influence carrier transport in addition to thermionic emission, the overall improvement in R_s, R_{sh}, and Φ_b confirms that 3% Sn incorporation enhances the electrical performance of the Schottky junction. These electrical findings are in good agreement with the structural (XRD) and optical (PL and UV–Vis) results, which demonstrate improved crystallinity and reduced defect density upon Sn doping.

3.3. Capacitance–Voltage and Conductance-Voltage Analysis (Kapasitans-Gerilim ve İletkenlik-Gerilim Analizi)

Based on the structural (XRD), optical (PL and UV–Vis), and current–voltage (I–V) analyses, the incorporation of 3% Sn is associated with improved crystallinity, modified defect characteristics, and enhanced rectifying behavior in the ZnO/n–Si Schottky structure. To further examine the electrical response of the optimized device, particularly in terms of charge distribution at the metal–semiconductor interface, depletion-region behavior, and frequency-dependent transport mechanisms, C–V and G/ω–V measurements were

Table 1. Extracted Schottky diode parameters (R_s, R_{sh}, n, and Φ_b) of Au/ZnO/n–Si and Au/ZnO:Sn (3%)/n–Si structures obtained from thermionic emission analysis (Termiyonik emisyon analizinden elde edilen Au/ZnO/n–Si ve Au/ZnO:Sn (3%)/n–Si yapılarının çıkarılan Schottky diyot parametreleri (R_s, R_{sh}, n ve Φ_b))

performed for the Au/ZnO:Sn (3%)/n–Si structure. Frequency dispersion in C–V and G/ω characteristics is commonly attributed to interface-state dynamics and barrier inhomogeneities in doped ZnO-based junction structures [6,18–20], thereby providing insight into interface-state response and AC transport behavior. It should be noted, however, that comparative C–V and G/ω measurements were not conducted for the undoped device; thus, while the observed interfacial characteristics are consistent with the structural and optical modifications introduced by Sn incorporation, a fully quantitative isolation of the Sn-specific contribution remains beyond the scope of the present study.

Figure 5 displays the C–V characteristics of the Au/ZnO:Sn (3%)/n–Si Schottky structure measured in the frequency range of 50 kHz to 1 MHz. In the negative-voltage region, the capacitance exhibits relatively low values, indicating the formation of a well-defined depletion region under reverse bias and confirming the Schottky-type junction behavior. The weak frequency dispersion observed in this region suggests that interface states are unable to effectively follow the applied AC signal at higher frequencies.

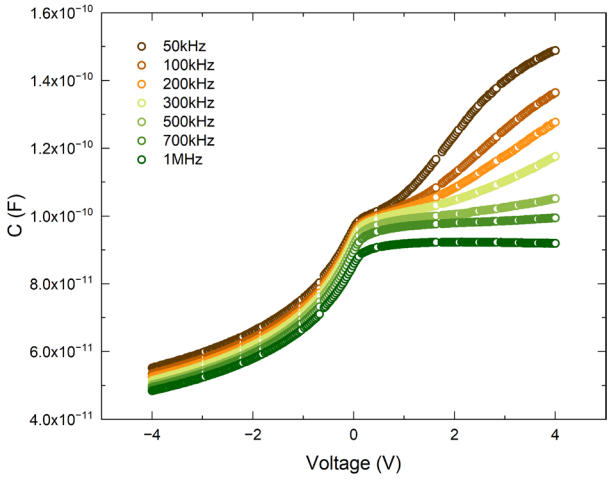


Figure 5. C–V results of the Au/ZnO:Sn (3%)/n-Si Schottky diode measured at frequencies ranging from 50 kHz to 1 MHz (50 kHz ila 1 MHz frekans aralığında ölçülen Au/ZnO:Sn (3%)/n-Si Schottky diyotunun C–V sonuçları)

Under forward bias, the capacitance increases and becomes more frequency dependent. The elevated capacitance values observed at lower frequencies can be attributed to the participation of interface states in charge-exchange processes, as these states can respond to the AC excitation. As the frequency increases, the measured capacitance decreases, indicating that the response of interface states becomes progressively suppressed and the depletion-layer capacitance dominates. This frequency-dependent behavior is characteristic of metal–semiconductor and doped ZnO-based junction structures, in which interface states exhibit finite response times [6,18].

The relatively smooth transition observed in the C–V curves suggest a comparatively uniform depletion-region modulation. When considered together with the reduced deep-level emission observed in PL measurements and the lower leakage current obtained from I–V analysis, the frequency-dependent capacitance response appears consistent with a stabilized interfacial behavior in the Sn-doped device. However, since corresponding C–V measurements were not performed for the undoped structure, the direct attribution of these interfacial characteristics solely to Sn incorporation should be interpreted in light of this experimental limitation.

Figure 6 shows the capacitance–frequency characteristics of the Au/ZnO:Sn (3%)/n–Si Schottky structure under different applied bias voltages (with a voltage step of 0.3 V). A monotonic decrease in capacitance with increasing frequency is observed across all bias conditions, a characteristic of Schottky-type junctions influenced by interface-state dynamics. Similar dispersion trends have been reported in doped ZnO-based MOS and thin-film junction structures, where the diminishing contribution of interface states at higher frequencies leads to convergence toward the depletion-layer capacitance [6].

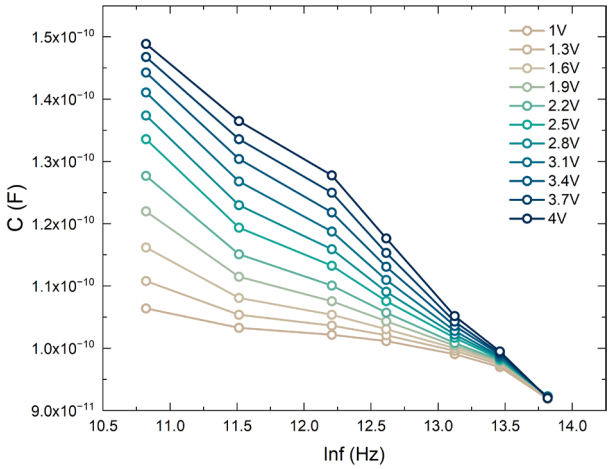


Figure 6. C–lnf results of the Au/ZnO:Sn (3%)/n-Si Schottky diode measured at different applied bias voltages (Farklı uygulanan ön gerilimlerde ölçülen Au/ZnO:Sn (3%)/n-Si Schottky diyotunun C–lnf sonuçları)

At lower frequencies, capacitance values are higher, particularly under forward bias, indicating that interface states can effectively respond to the AC signal. As the frequency increases, the capacitance

curves converge, suggesting that the electrical response becomes increasingly governed by the intrinsic junction properties rather than interface-related contributions. These observations are consistent with a controlled interface-state response in the examined structure, although a direct comparative analysis with the undoped device would be required for a fully quantitative assessment of the role of Sn incorporation.

The G/ω–V characteristics of the Au/ZnO:Sn (3%)/n–Si Schottky structure measured at different frequencies are presented in Figure 7. In the reverse-bias region, the G/ω values remain relatively low and show minimal variation with applied voltage, indicating that AC conductance is primarily governed by the depletion region with limited trap-assisted conduction. As the applied voltage shifts toward forward bias, a noticeable increase in G/ω is observed, especially at lower frequencies. This increase suggests enhanced participation of interface states in charge-exchange processes when the AC signal can be tracked. At higher frequencies, the conductance response is suppressed, consistent with the finite response time of interface states. Comparable conductance dispersion behavior associated with interface-state dynamics has been reported in doped ZnO-based junctions and MOS structures [6].

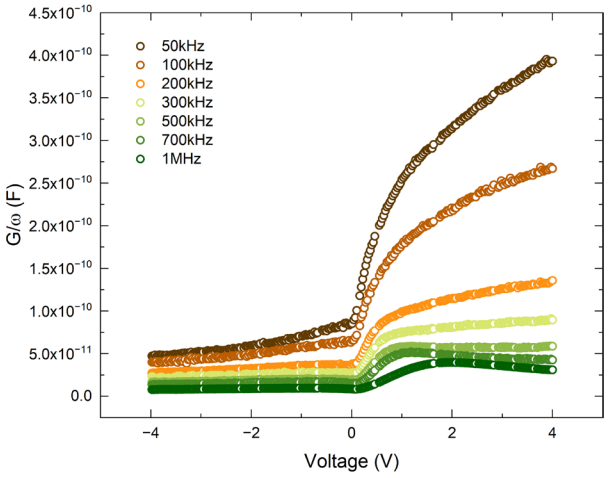


Figure 7. G/ω–V results of the Au/ZnO:Sn (3%)/n-Si Schottky diode measured (Au/ZnO:Sn (3%)/n-Si Schottky diyotunun ölçülen G/ω–V sonuçları)

Overall, the G/ω–V behavior supports the presence of frequency-dependent interface-state activity and depletion-region–controlled transport. While these characteristics are consistent with the structural and optical improvements observed in the Sn-doped film, the absence of corresponding measurements for the undoped device limits a definitive isolation of the Sn-specific contribution.

Figure 8 presents the G/ω–f characteristics of the Au/ZnO:Sn (3%)/n–Si Schottky structure under different applied bias voltages (with a voltage step of 0.3 V). A systematic decrease in G/ω with increasing frequency is observed under all bias conditions. This trend is typically attributed to the finite response time of interface states, whose contribution diminishes as frequency increases. A similar frequency-dependent conductance suppression has been reported in doped ZnO thin films and MOS-type structures [6,18].

At lower frequencies, G/ω values are higher and increase under forward bias, indicating more pronounced charge-exchange processes at the interface. As the frequency increases, the curves converge toward lower conductance values, suggesting that the junction's intrinsic properties dominate the high-frequency regime. Taken together, the C–V and G/ω analyses indicate a frequency-dependent interface response and a stable depletion-region modulation in the Au/ZnO:Sn (3%)/n–Si structure. These findings are consistent with the reduced defect-related recombination inferred from PL and the improved rectifying behavior observed in I–V measurements. Nevertheless, a fully quantitative evaluation of the specific contribution of Sn incorporation would require comparative measurements on the undoped structure.

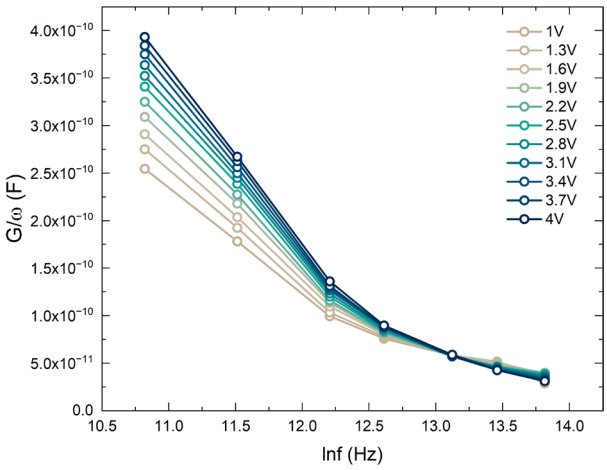


Figure 8. G/ω–lnf results of the Au/ZnO:Sn (3%)/n-Si Schottky diode measured under different applied bias voltages (Farklı uygulanan ön gerilim altında ölçülen Au/ZnO:Sn (3%)/n-Si Schottky diyotunun G/ω–lnf sonuçları)

In general terms, the C–V characteristics measured over 50 kHz to 1 MHz exhibit typical Schottky behavior. In the reverse-bias region, relatively low capacitance values indicate the formation of a well-defined depletion region. The weak frequency dependence in this region suggests that interface

states are unable to effectively follow the applied AC signal at higher frequencies. Under forward bias, the capacitance increases and shows noticeable frequency dispersion, particularly at lower frequencies. This behavior indicates that interface states can respond to the AC signal and participate in charge exchange processes. As the frequency increases, the capacitance gradually decreases, and the curves converge, implying that the measured response becomes increasingly dominated by the depletion-layer capacitance rather than interface-related contributions. Similar forward-bias capacitance dispersion and interface-state related admittance features have been reported in doped ZnO interlayer Schottky and metal-insulator-semiconductor (MIS) structures [19,20].

The G/ω–V characteristics further support this interpretation. In the reverse-bias region, G/ω values remain relatively low and show minimal voltage dependence, suggesting that trap-assisted conduction is limited. As the applied voltage shifts toward forward bias, G/ω increases, especially at lower frequencies, revealing enhanced interface-state activity and charge exchange at the metal–semiconductor boundary. With increasing frequency, the G/ω response is progressively suppressed, confirming that interface states cannot effectively track high-frequency AC signals. Comparable frequency-dependent conductance suppression attributed to limited interface-state response time has also been documented in doped ZnO-based MS and MIS configurations [19,20].

Overall, the admittance analysis indicates that the Sn-doped ZnO/n–Si structure exhibits stable depletion-region behavior, limited active interface-state density within the measured frequency window, and improved AC electrical response. Although a direct comparison with the undoped device is not available, the combined structural, optical, and electrical findings consistently suggest that Sn incorporation enhances interfacial stability and reduces defect-assisted conduction mechanisms.

4. CONCLUSIONS (SONUÇLAR)

In this study, undoped and 3% Sn–doped ZnO thin films were fabricated by RF magnetron co-sputtering, and the structural, optical, and electrical properties of Au/ZnO/n–Si and Au/ZnO:Sn (3%)/n–Si Schottky diodes were comprehensively investigated. XRD analysis confirmed that both films crystallized in the hexagonal wurtzite phase with a pronounced (002) preferred orientation. The incorporation of 3% Sn preserved the single-phase structure while enhancing crystalline quality, as evidenced by increased (002) peak intensity, enlarged crystallite size, and reduced microstrain.

Photoluminescence results showed that Sn incorporation enhanced near-band-edge emission and suppressed deep-level emission, thereby increasing the I_{NBE}/I_{DLE} ratio. This behavior indicates a reduction in defect-related non-radiative recombination centers and is consistent with the structural improvements observed in XRD analysis. UV–Visible spectroscopy demonstrated high optical transmittance in the visible region, while Tauc analysis revealed a slight modification of the optical band structure upon Sn doping. These findings collectively highlight the role of Sn in defect engineering within ZnO thin films.

Current–voltage measurements confirmed Schottky-type rectifying behavior in both structures; however, the Sn-doped device exhibited superior electrical performance. The improvement was reflected in increased barrier height, reduced series resistance, a lower ideality factor, and enhanced forward current conduction. These enhancements are attributed to increased donor concentration, improved crystallinity, and reduced interface defect density.

Admittance analysis (C–V, C–f, G/ω–V, and G/ω–f), performed on the Au/ZnO:Sn (3%)/n–Si structure, indicated stable depletion-region behavior, limited active interface-state response within the measured frequency range, and improved AC transport characteristics. Although comparative admittance measurements were not conducted for the undoped structure, the combined structural, optical, and electrical findings consistently support the beneficial role of Sn incorporation in enhancing interfacial stability and suppressing defect-assisted conduction mechanisms.

Overall, 3% Sn incorporation into ZnO thin films produced by RF magnetron sputtering simultaneously improves crystalline quality, defect-related optical behavior, and Schottky junction performance. The resulting Au/ZnO:Sn (3%)/n–Si device, characterized by low leakage current and stable high-frequency response, represents a promising candidate for UV detection and optoelectronic rectifier applications. Future studies may focus on systematic optimization of Sn concentration and advanced interface engineering strategies to further clarify and enhance the structure–property–device performance relationship.

ACKNOWLEDGMENTS (TEŞEKKÜR)

This study was supported by the Directorate of the Presidential Strategy and Budget of Turkey (Project No: 2019K12-149045). I would like to thank the director and staff of the Gazi University Photonics Application and Research Center for their valuable contributions to this study. / Bu çalışma, Türkiye Cumhurbaşkanlığı Strateji ve Bütçe Başkanlığı tarafından desteklenmiştir (Proje No: 2019K12-149045). Bu çalışmaya değerli katkıları için Gazi Üniversitesi Fotonik Uygulama ve Araştırma Merkezi müdürü ve çalışanlarına teşekkür ederim.

DECLARATION OF ETHICAL STANDARDS (ETİK STANDARTLARIN BEYANI)

The author of this article declares that the materials and methods they use in their work do not require ethical committee approval and/or legal-specific permission.

Bu makalenin yazarı çalışmalarında kullandıkları materyal ve yöntemlerin etik kurul izni ve/veya yasal-özel bir izin gerektirmediğini beyan ederler.

AUTHORS' CONTRIBUTIONS (YAZARLARIN KATKILARI)

***Erman ÇOKDUYGULULAR*:** A single author conducted the present study.

Bu çalışma tek bir yazar tarafından yürütülmüştür.

CONFLICT OF INTEREST (ÇIKAR ÇATIŞMASI)

There is no conflict of interest in this study.

Bu çalışmada herhangi bir çıkar çatışması yoktur.

REFERENCES (KAYNAKLAR)

[1] M. Willander, O. Nur, J.R. Sadaf, M.I. Qadir, S. Zaman, A. Zainelabdin, N. Bano, I. Hussain, Luminescence from zinc oxide nanostructures and polymers and their hybrid devices, Materials 3 (2010) 2643–2667. https://doi.org/10.3390/ma3042643.

[2] J.A. Röhr, J. Sá, S.J. Konezny, The role of adsorbates in the green emission and conductivity of zinc oxide, Commun. Chem. 2 (2019). https://doi.org/10.1038/s42004-019-0153-0.

[3] S. Bhatia, N. Verma, R.K. Bedi, Sn-doped ZnO nanopetal networks for efficient photocatalytic degradation of dye and gas sensing applications, Appl. Surf. Sci. 407 (2017) 495–502. https://doi.org/10.1016/j.apsusc.2017.02.205.

[4] V. Ganesh, I.S. Yahia, S. AlFaify, M. Shkir, Sn-doped ZnO nanocrystalline thin films with enhanced linear and nonlinear optical properties for optoelectronic applications, Journal of Physics and Chemistry of Solids 100 (2017) 115–125. https://doi.org/10.1016/j.jpcs.2016.09.022.

[5] A.Z. Ahmed, M.M. Islam, M.M. ul Islam, S.M. Masum, R. Islam, M.A.I. Molla, Fabrication and characterization of B/Sn-doped ZnO nanoparticles via mechanochemical method for photocatalytic degradation of rhodamine B, Inorganic and Nano-Metal Chemistry 51 (2020) 1369–1378. https://doi.org/10.1080/24701556.2020.1835976.

[6] E. Çokduygulular, Ç. Çetinkaya, Y. Yalçın, B. Kınacı, A comprehensive study on Cu-doped ZnO (CZO) interlayered MOS structure, Journal of Materials Science: Materials in Electronics 31 (2020) 13646–13656. https://doi.org/10.1007/s10854-020-03922-6.

[7] S. Ameen, M.S. Akhtar, H.K. Seo, Y.S. Kim, H.S. Shin, Influence of Sn doping on ZnO nanostructures from nanoparticles to spindle shape and their photoelectrochemical properties for dye sensitized solar cells, Chemical Engineering Journal 187 (2012) 351–356. https://doi.org/10.1016/j.cej.2012.01.097.

[8] H. Aydin, H.M. El-Nasser, C. Aydin, A.A. Al-Ghamdi, F. Yakuphanoglu, Synthesis and characterization of nanostructured undoped and Sn-doped ZnO thin films via sol-gel approach, in: Appl. Surf. Sci., Elsevier B.V., 2015: pp. 109–114. https://doi.org/10.1016/j.apsusc.2015.02.189.

[9] N. Chahmat, T. Souier, A. Mokri, M. Bououdina, M.S. Aida, M. Ghers, Structure, microstructure and optical properties of Sn-doped ZnO thin films, J. Alloys Compd. 593 (2014) 148–153. https://doi.org/10.1016/j.jallcom.2014.01.024.

[10] A. Yildiz, E. Ozturk, A. Atilgan, M. Sbeta, A. Atli, T. Serin, An Understanding of the Band Gap Shrinkage in Sn-Doped ZnO for Dye-Sensitized Solar Cells, J. Electron. Mater. 46 (2017) 6739–6744. https://doi.org/10.1007/s11664-017-5778-0.

[11] M. Ajili, M. Castagné, N.K. Turki, Study on the doping effect of Sn-doped ZnO thin films, Superlattices Microstruct. 53 (2013) 213–222. https://doi.org/10.1016/j.spmi.2012.10.012.

[12] R. Yousefi, Effects of Sn atoms on formation of ZnO nanorings, CrystEngComm 17 (2015) 2698–2704. https://doi.org/10.1039/c5ce00316d.

[13] M. Kumar, V. Bhatt, A.C. Abhyankar, J. Kim, A. Kumar, J.H. Yun, Modulation of structural properties of Sn doped ZnO for UV photoconductors, Sens. Actuators A Phys. 270 (2018) 118–126. https://doi.org/10.1016/j.sna.2017.12.045.

[14] S. Johnson Jeyakumar, J. Vasudevan, B. Arunkumar, M. Jothibas, A. Rajeswari, R. Sathiskumar, A. Muthuvel, Structural, optical and magnetic behavior of Sn doped ZnO nanoparticles prepared by solid state method, in: Mater. Today Proc., Elsevier Ltd, 2019: pp. 371–376. https://doi.org/10.1016/j.matpr.2020.09.376.

[15] N. Venkatesh, S. Aravindan, K. Ramki, & Govindhasamy Murugadoss, R. Thangamuthu, P. Sakthivel, Sunlight-driven enhanced photocatalytic activity of bandgap narrowing Sn-doped ZnO nanoparticles, (n.d.). https://doi.org/10.1007/s11356-020-11763-3/Published.

[16] S. Selvinsimpson, P. Gnanamozhi, V. Pandiyan, M. Govindasamy, M.A. Habila, N. AlMasoud, Y. Chen, Synergetic effect of Sn doped ZnO nanoparticles synthesized via ultrasonication technique and its photocatalytic and antibacterial activity, Environ. Res. 197 (2021). https://doi.org/10.1016/j.envres.2021.111115.

[17] B. Abdallah, W. Zetoun, A. Tello, Deposition of ZnO thin films with different powers using RF magnetron sputtering method: Structural, electrical and optical study, Heliyon 10 (2024). https://doi.org/10.1016/j.heliyon.2024.e27606.

[18] S. Ishak, S. Johari, M.M. Ramli, Formaldehyde detection using Sn doped ZnO thin film, J. Solgel Sci. Technol. 95 (2020) 265–275. https://doi.org/10.1007/s10971-020-05318-8.

[19] A. Demirci, H.G. Çetinkaya, P. Durmuş, S. Demirezen, Altındal, Optoelectronic characterization of Bi-doped ZnO nanocomposites for Schottky interlayer applications, Physica B Condens. Matter 670 (2023). https://doi.org/10.1016/j.physb.2023.415338.

[20] S. Çolak, S. Demirezen, Iron phthalocyanine(FePc)-sensitized ZnO for enhanced photovoltaic and electronic performance, Phys. Scr. 100 (2025) 105968. https://doi.org/10.1088/1402-4896/ae13c6.